

INVITED PAPER

Ultrafast–ultrafine probing of high-speed electrical waveforms using a scanning force microscope with photoconductive gating

J. NEES

*University of Michigan, Center for Ultrafast Optical Science, 1006 IST Bldg.,
2200 Bonisteel, Ann Arbor, MI 48 109-2099, USA*

S.-I. WAKANA, S. HAMA

*Fujitsu Laboratories Ltd, 1-10 Morinosato, Wakamiya Atsugi,
Kanagawa 243-01, Japan*

Received 29 November 1995; revised 18 January, accepted 26 January 1996

Picosecond photoconductivity in low-temperature-grown GaAs (LT GaAs) has been used to provide temporal resolution both in rigid probes and in scanning force microscope probes. This article reviews the fabrication and use of such probes. 2.5 ps temporal resolution and few microvolts sensitivity are obtained at arbitrary points on circuits with a spatial definition of 100 nm. Rigid probes are tested in application to analogue and digital circuits. As an alternative to electron beam testing, scanning force probes are applied to *in situ* imaging and waveform measurement. Finally, the use of time-resolved waveform analysis with scanning-force microscopy probes with semiconductor laser sources is demonstrated.

1. Introduction

In recent decades the emergence of the personal computer industry and the expansion of the telecommunications industry have carried the development of integrated circuit technologies to astonishing lengths. Anticipation of advanced technologies and new market directions has become key to the viability of both products and companies in these markets. Even long established companies have employed dramatic measures to bring about faster implementation of new designs.

In this environment a clear understanding of circuit operation is critical to producing functional devices and systems on the first run of a new design. Information from previous devices must be harvested to add power to models for new circuits. Analysis of functionality limits within devices can provide valuable information for increasing the upper bound of operation and for avoiding costly mistakes in production.

Direct time-resolved investigation of the internal functionality of very large-scale integration (VLSI) circuits has been carried out by a small number of methods. Voltage contrast imaging

has been integrated into complete electron-beam test systems which have the capability to image circuits and to measure and compare waveforms [1, 2]. Owing to the complexity of working in vacuum and the difficulty of obtaining high signal-to-noise ratios, new methods for testing VLSI have been under investigation for more than a decade. A second form of internal-node sampling which has been developed to produce fine temporal resolution in integrated circuit testing is electrooptic sampling [3, 4]. Utilizing the fine temporal resolution afforded by pulsed lasers, measurements of 200 fs resolution have been made [5]. While this technique is powerful in obtaining fine temporal resolution, it is limited in its ability to deliver the fine spatial resolution of the scanning electron microscope [6].

With a compromise in the scan-rate of the electron microscope and the temporal resolution of electrooptic sampling an alternative measurement technique has emerged which provides submicrometre spatial resolution and picosecond temporal resolution with high sensitivity. Spatial resolution is derived from a scanning force microscope and temporal resolution is provided by a photoconductive (PC) gate integrated on the force-sensing cantilever. These elements provide a sensitivity in the range of few microvolts per square root hertz. This paper describes the use of the PC effect to sample waveforms at points internal to working circuits [7]. Also, the adaptations used to fit a commercial scanning force microscope with picosecond-waveform-measurement capability are detailed and the limitations of such imaging waveform analysers are discussed.

2. Building blocks for ultrafast PC probes

2.1. Photoconductivity

The PC effect [8] is used primarily in three high-speed applications: detection of optical signals, power switching, and gating of electronic signals. As it is implemented to detect optical radiation a photoconductor is typically biased with as large an electric field as possible; in the velocity saturation regime and safely below breakdown due to impact ionization. This maximizes the signal from relatively low light levels. In this configuration the linearity of the detector current with respect to bias field is of no concern. In power switching applications both the bias and the optical switching power are maximized to yield high power output from the PC switch. As a gate the photoconductor is devised to maintain high resistance in the off-state and moderate to low resistance in the on-state. It is likely to be switched with higher optical power, while the electric field bias may vary. In any of these functions the duration of the photoconductivity is governed by the lifetime of the carriers in the semiconductor.

2.2. High-speed PC materials

Semiconductor material systems with picosecond carrier lifetime are not uncommon. Most amorphous materials have high densities of traps at the grain boundaries. Unfortunately these materials also have very poor mobility, low breakdown potential and significant dark-conductivity. Traditionally picosecond and femtosecond carrier lifetimes have been obtained in silicon-on-sapphire (SOS) by ion implantation [9]. This produces short carrier lifetime and high resistivity, but the mobility which governs the saturated velocity of carriers is still quite low. This results in lower current for a given optical excitation energy. While a sample of semi-insulating GaAs may display a mobility of $8000 \text{ cm}^2 \text{ V}^{-1} \text{ s}^{-1}$, implanted SOS with sub-picosecond lifetime produces a mobility of a few tens of centimetres squared per volt per second. More recently the discovery of non-stoichiometric III-V materials has led to the development of femtosecond-lifetime materials with mobilities of a few hundred centimetres

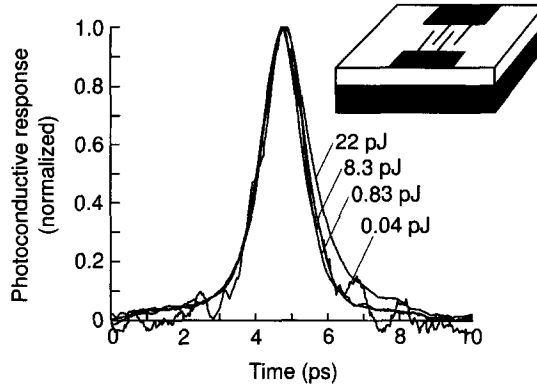


Figure 1 Impulse response of $7 \times 8 \mu\text{m}$ MSM with $0.2 \mu\text{m}$ finger spacing, illuminated by 100 fs, 620 nm pulses. Measured by Gupta *et al.* [13].

squared per volt per second [10, 11]. The foremost of these materials is GaAs grown at reduced temperatures ($\sim 200^\circ\text{C}$) by molecular beam epitaxy (LT GaAs).

Lifetimes of free carriers in semiconductor materials such as these are measured by time-resolved reflectivity. In this measurement ion-implanted SOS displays a reflectivity change for a period of less than 1 ps following illumination by 120 fs pulses of 810 nm light at $5 \times 10^6 \text{ W cm}^{-2}$ power density. This time-resolved reflectivity is an indicator of free carrier concentration on the surface of the SOS sample and of a subpicosecond carrier lifetime. Short carrier lifetime is exhibited in LT GaAs both in the as-grown state and after annealing at the normal growth temperature of 600°C for 10 min. While research into the nature of the carrier transport in LT GaAs is ongoing, the favourable characteristics of reasonably high mobility, high breakdown potential, and high dark-resistance are all available in this GaAs system. These qualities can be exploited to make an efficient high-speed gate for sampling electrical signals on arbitrary circuits [12]. Figure 1 shows the response of an LT GaAs metal–semiconductor–metal structure with finger spacing and finger width of $0.2 \mu\text{m}$ and an area of $7 \times 8 \mu\text{m}$ [13]. This PC switch has an on-state resistance, R_{on} , of as low as 30Ω under 22 pJ, 100 fs pulse illumination at 620 nm. In the off-state it maintains $\text{G} \Omega$ resistance, R_{off} .

2.3. Detection electronics

Detection of the weak signal sampled from a repeating waveform has been accomplished by low impedance and high impedance electronics yielding similar results. Where high impedance electronics are used the charge sampled from the high-speed waveform is stored in the capacitance of a lock-in amplifier or a high-resistivity field-effect transistor (FET) amplifier [14, 15]. A simple diagram showing the key elements of the test electronics is shown in Fig. 2. As the gate samples additional charge from the test circuit the voltage on the storage capacitor builds up to the unknown transient level. When these two voltages are equal no more charge is transferred and the voltage across the lock-in or FET amplifier nearly equals the momentary voltage at the sampling point. The accuracy of the measurement technique is limited by the dark current of the PC gate and by the conductivity of the lock-in or amplifier reading the storage capacitor. In this scheme the electronic signal or the light enabling the sampling gate must be chopped at a rate which allows the storage capacitor to come to equilibrium with the transient voltage within each cycle. With higher chopping rates, in the regime

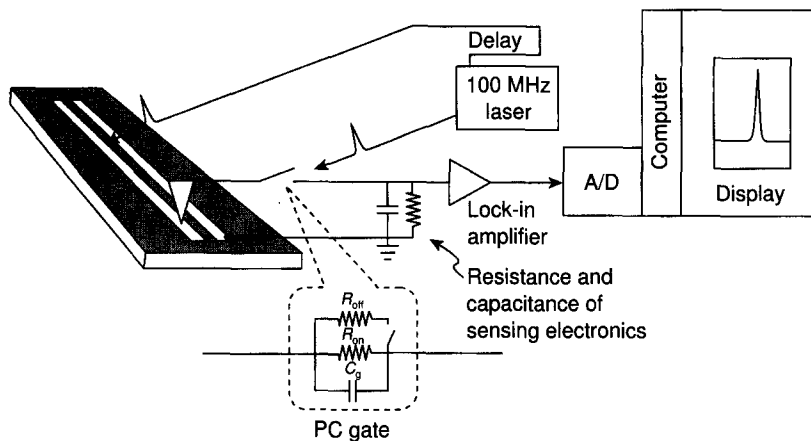


Figure 2 Schematic diagram of electronics used to acquire waveforms using PC probes. R_{off} , R_{on} , and C_g are the off-state resistance of the PC gate, its on-state resistance and its gap capacitance, respectively.

where the potential across the storage capacitor remains much less than the sampled potential, the signal level is reduced in proportion to the chopping interval.

Alternatively, low impedance detection electronics have been used to acquire signals from PC sampling gates. This configuration places the entire test signal potential across the gate. Using electronics with bandwidth in excess of the sampling rate allows single-shot measurement of sampled signals to be made. This configuration also presents a greater challenge to the linearity of the measurement system. This can arise from the saturation of the drift velocity of carriers in the sampling gate. High bandwidth detection electronics are also more sensitive to the small transient signals coupled from the test device by the PC-gap capacitance, C_g . The photovoltaic effect is present at metal semiconductor junctions due to the presence of charge depletion near the metal contact. In many material systems ohmic contacts can be made by reducing the Schottky region to the point where current can readily tunnel through. As a result of the extremely low free-carrier population in LT GaAs there is no clear way to form ohmic contacts on this material. This poses the problem in measurements where the photovoltaic current carries with it the frequency, $1/f$, noise of the laser beam. In measurements of VLSI circuits where a few fC of charge may be crucial to the device's operation the probe could launch such charge onto the device. The effect of the photovoltaic signal may also be quite large in comparison to the desired signal. This necessitates additional steps of calibration. Though these transients include no drift current, their induced current may exceed the sampling current by more than an order of magnitude.

Low impedance detection electronics can have an advantage in that they conduct the sampled transients away from the sampling gate. By maintaining a constant impedance on the back side of the sampling gate reflections which could interfere with the value of subsequent samples (for high sampling rates) can be matched to the detecting amplifier.

2.4. Considerations of the proximity of the gate to the test-point

The possibility of reflections occurring on the front side of the gate (the side connected to the test sample) must also be considered in the probe design. From the perspective of the time domain, PC sampling probes will split the power of transients propagating on a test sample

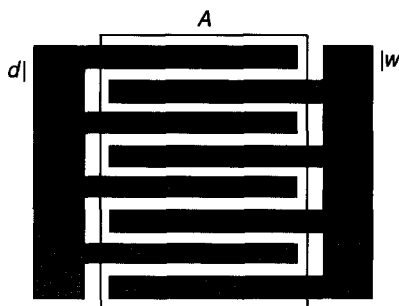


Figure 3 Interdigital finger configuration used in calculating gap capacitance, C_g .

between their normal path and a new path to the sampling gate. The existence of any time delay between the test-point and the sampling gate will cause the reflection of the deviated signal to interfere with the undeviated signal. Microwave circuit design requires that the path between the test-point and the gate be less than one-eighth of the wavelength of the highest frequency within the 3 dB measurement bandwidth. A spacing of less than $100 \mu\text{m}$ is required for picosecond transients with 350 GHz bandwidth.

2.5. High-speed PC gates

The capacitance of the PC gate must be considered from the standpoint of the load it places on the test circuit. For signals of 350 GHz bandwidth a PC gate with a $2 \times 2 \mu\text{m}^2$ gap having a capacitance, C_g , of 1 fF presents a $1/\omega C$ load of only 450Ω to the highest frequencies. Interdigital MSMs are often preferred to simple-gap MSMs for ease of alignment. The following is a formula for the capacitance of an MSM on a material with dielectric constant, ϵ_r [16]:

$$C = K(k)/K(k')\epsilon_0(1 + \epsilon_r)A/d$$

Here

$$k = \tan^2(\pi w/4d)$$

$$k' = (1 - k^2)^{1/2}$$

$K(k)$ is the elliptic integral of the first kind, A is the interdigital area, w is the finger width, and d is the centre-to-centre spacing of the fingers, as in Fig. 3.

The interdigital design may also be used to enhance the responsivity of the PC switch. This is true because the number of electrons which are captured by the positive contact in the MSM on short lifetime material is inversely proportional to the gap width. If the gap width is set so that electrons with saturated drift velocity can traverse the gap during the carrier lifetime virtually all the excited carriers will be detected. With gap lengths larger than this a certain portion of the photoelectrons will not contribute to the detected current. For LT GaAs a gap of $0.2 \mu\text{m}$ is necessary to meet this condition. The response of such detector-gates has been measured by Chen *et al.* [13]. Following the demonstration of efficient gating, LT GaAs MSMs were used to make free-standing PC probes.

2.6. Formation of free-standing PC probes

In conventional use PC gates have been fabricated in or beside electronic devices and structures. A PC *probe* is a two-terminal PC gate with one, sensing, electrode fitted to contact

electronic circuits. The second electrode communicates sampled signals to acquisition electronics. It is also necessary for the substrate on which the gate and electrodes are formed to be separated from its host wafer. Once the probe is freely positionable it can be placed in contact with the desired location on a test circuit and optically triggered to analyse the circuit's electrical behaviour. The properties of these probes and tests using them will be described in Section 4. While these probes proved useful in testing high-speed devices, the prospect of combining the time-resolution they demonstrate with scanning microscopy has generated a great deal more interest.

2.7. A PC probe with scanning force microscope capability

Scanning probe microscopy has made it possible to obtain submicrometre spatial resolution outside of vacuum. While a rich variety of probes are used in research most of the probes fit into three main categories based on the type of sample-probe interaction. These are near-field scanning optical microscopes, scanning tunnelling microscopes and scanning force microscopes (SFM, often called atomic force microscopes due to the minute scale of the forces involved). Scanning force microscopy is the easiest of the three to use. Indeed, it is typically used to control the position of near-field optical probes. Commercial SFM systems are available from numerous companies in the price range from US\$15 000 to 100 000 (1996 prices).

Typical SFM probes have cantilevers extending between 100 and 500 μm from their base with submicrometre thickness. At the free end of the cantilever is a tip which interacts with the test sample. These conical or pyramidal tips rise from the surface of the cantilever by a few micrometres to a fine point with nanometre radius. Together the tip and cantilever form a stylus. The SFM system measures the force exerted on the micro-stylus as it interacts with the surface of a material by sensing the deflection of a continuous wave (CW) laser beam reflected from the cantilever. As the stylus is scanned across the surface of a test sample, the variation in the force on the tip is translated into a feedback signal which is programmed to maintain constant force by moving the base of the probe in the z -direction (toward or away from the sample). By recording the magnitude of the voltage required to position correctly the base of the stylus, while the probe is scanned in x - and y -directions, a raster-image of the surface is produced.

In order to use the tip of a scanning force probe to make electrical contact with the test circuit the tip must be conductive. As stated in the discussion on proximity, the tip must also be located within 100 μm of the PC gate if picosecond resolution is desired. While it is not feasible to fix a photoconductor onto commercial probe cantilevers, it is possible to fabricate the cantilever from epitaxially grown materials such as LT GaAs. To use the epitaxial layer without its host substrate has the added benefit that the gating light pulses can be passed through the micrometre-thick semiconductor to the PC switch. The process by which these probes are fabricated involves the formation of the photogate, the formation of a sharp tip, and the release of the epitaxial material from its host wafer.

3. Tools for probe formation

A standard set of recipes is necessary when any microlithographic process is to be done. The elements of GaAs processing differ substantially from those used in Si processing, both in composition and in variety. The component processes of probe formation occur in a few major categories. These are: molecular-beam-epitaxy (MBE) growth, patterning, thin-film deposition, etching, self-terminating tip formation, and assembly.

3.1. MBE growth

LT GaAs is the key component to the time resolution of the SFM probe. This material is formed, at present, only by the MBE process. The range of growth temperatures for this material is from 190 to 300°C. Following growth at reduced temperatures the wafer is annealed at 600°C for 10 min.

In addition to the growth of this layer it is also necessary to grow a second layer with chemical properties substantially differing from those of GaAs to create an etch barrier. In most of the work Ga_{0.5}Al_{0.5}As was used for this purpose.

3.2. Patterning

Photoresist is used, as in silicon processing, to define areas of the processed wafer for exposure to metal or dielectric deposition or exposure to etchants. The patterning processes used employ the following recipes:

3.2.1. Positive patterning

Spin on photoresist; soft-bake for 1 min; soak in chlorobenzene (a strong carcinogen) for 7 min; hard-bake for 1 min; expose; develop; evaporate or etch; remove by soaking in acetone.

3.2.2. Reverse field patterning

Spin on photoresist; hard-bake for 1 min; expose; post-bake for 1 min; develop; hard-bake for 10 min; evaporate or etch; remove by soaking in acetone.

3.2.3. Thin-film deposition

Different forms of the SFM probe require metallic, semiconductor and dielectric thin films. Metal films may be deposited by e-beam evaporation or by sputtering. E-beam evaporation was used primarily due to the high degree of directionality.

3.3. Etching

Beside their utility in patterning, etchants are also valuable for removing unwanted substrate material or for freeing thin-film elements from their host substrate. When etchants are used to free portions of epitaxially grown layers from their host substrate it is necessary to have a layer which can protect wanted parts or act as a sacrificial layer to allow particular parts to be released from the host substrate. A wide variety of chemicals are available which have the capability to select between metals and dielectrics of different types and semiconductors. A smaller selection is available to select between different layers in a compound semiconductor group, such as Ga_xAl_{1-x}As. Then there are a few instances where a significant selectivity in etch direction can be found.

In processing the GaAs/Ga_{0.5}Al_{0.5}As system a complete set of etchants exists. To dissolve the GaAs while leaving the Ga_{0.5}Al_{0.5}As undisturbed a solution of NH₄OH:H₂O at a ratio of 1:24 is used to remove material at 5–7 μm min⁻¹. While this is effective for removing the 500 μm thick bulk of the GaAs substrate, samples are generally thinned to 100 μm thickness before this etch. To remove Ga_{0.5}Al_{0.5}As while leaving GaAs unchanged, a solution of 10% by mole HF:H₂O is used. Finally, to etch both materials HP₃O₄:H₂O₂:H₂O at 3:1:25 is used to remove 0.2 μm min⁻¹. When SiO₂ is used as a dielectric on GaAs, HF is used as a selective etch.

3.4. Self-terminating tip formation

Various methods of forming tips for SFM are in use today. These silicon-based technologies

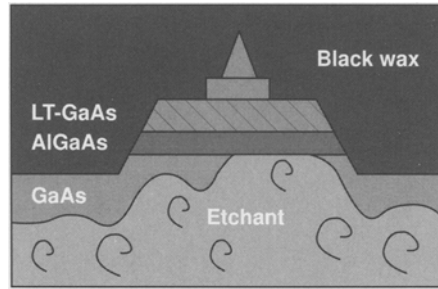


Figure 4 Illustrated cross-section of the probe-tip during back-side etch. The dark AlGaAs layer provides an etch barrier to the GaAs etchant.

use anisotropic etching of silicon to form a tip or to form a mould for a tip. Alternatively, tips may be formed by using an etchant to under-cut a small cover area, leaving a fine tip as the support for the cover is gradually dissolved. These methods do not have direct application to the formation of sharp tips on GaAs substrates. The technique for fabricating the metallic tip on GaAs is borrowed from the field of vacuum-microelectronics [17]. Using a lift-off process, a circular hole is patterned in photoresist; metal is evaporated onto the wafer and adheres to both photoresist and substrate; as the thickness of the metal increases during growth the circular aperture closes, narrowing the aperture and hence the diameter of the metal adhering to the substrate encompassed by the circular aperture. This process eventually closes the hole leaving a sharp conical tip buried, as illustrated in Fig. 4. The critical feature of the process is that the tip is in no place in contact with other metallizations. Therefore, when the photoresist is removed, only the tip remains: the upper metal layer washes away with photoresist which supports it. The adaptation of this process from a silicon-based process involving SiO_2 first involved sputtering, but this yielded tips with $1\ \mu\text{m}$ radii. Using e-beam evaporation several metals

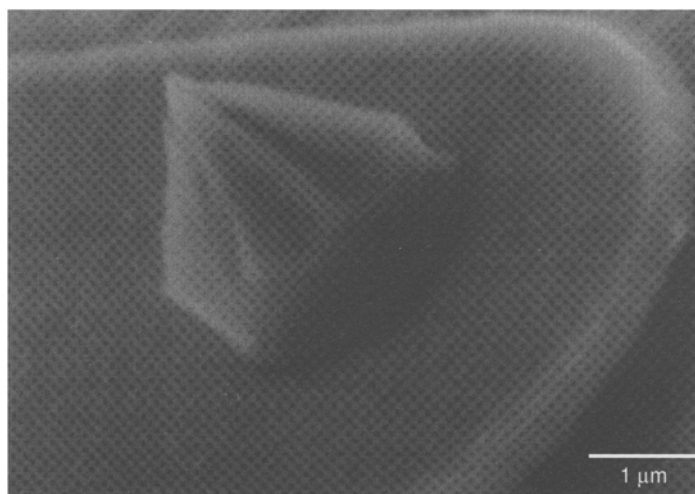


Figure 5 Scanning electron micrograph of a Ti tip formed by self-terminating lift-off.

including Au, Al and Ti have been tested. Each metal has a characteristic angle of inclination. Ti, shown in Fig. 5, makes a tip with a $70\text{--}80^\circ$ included angle, while the angle for Au is at the order of $40\text{--}60^\circ$.

3.5. Assembly

Using the above tools one is able to make probes ranging from bulk probes, with dull tips and amorphous semiconductor switches, to fibre-supported LT GaAs probes with tip-radii of $0.1\ \mu\text{m}$. Individual probe styles will be described later, along with other applications, advantages and disadvantages. There are a few elements common to the assembly of these probes.

In general the probe tips are formed on the under side of the probe, i.e. the side which faces the test circuit. The fact that the authors' probes are at the order of $5\ \text{mm}$ to $300\ \mu\text{m}$ combined with the fact that, in use, the angle between the probe face and the surface under test is not more than 15° , requires that no thick wires or tall wire-bond loops be raised between the probe and the test circuit. Silver paint and silver epoxy were typically used to make connections to the probes, as these materials can be made to lay close to the surfaces they bond.

Some of the probe structures require that a $1\ \mu\text{m}$ thick LT GaAs crystal be bonded to a glass substrate or fibre. These mechanical connections are made using ultraviolet (UV) curing cement. In order not to deform the thin crystal only a few picolitres of adhesive can be used. This amount is controlled by dabbing excess glue from a needle tip onto other surfaces. When this is done and the thin crystals are mounted there is little opportunity to move the probe without damaging it. Cyanoacrylate or 'super glue' is used to bond components of the probe base together.

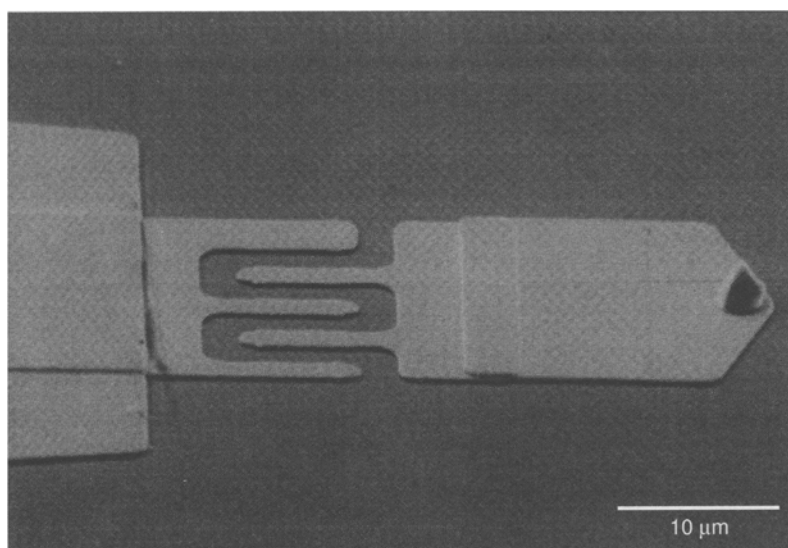


Figure 6 Scanning electron micrograph of a rigid probe with a $100\ \text{nm}$ tip radius. In experiments with rigid probes larger-area pads are preferred for their better adhesion.

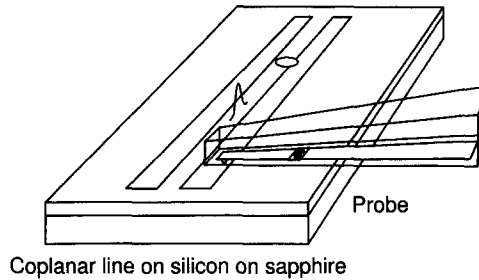


Figure 7 Configuration of the rigid probe in measuring its impulse response.

4. Forming freely positionable bulk probes

Using photolithography to define an interdigital switch and a few micrometre thick metal pad probe structures are formed on LT GaAs or SOS. Figure 6 shows a scanning electron micrograph of such a probe. This leaves the problems of freeing the probes and illuminating the PC switches. A wafer saw can be used to cut apart probes of submillimetre width leaving the contacting pad near one of the two edges so the probe can be tilted slightly with respect to the circuit under test. Activation of the gate on SOS is accomplished by directing pulsed light through the sapphire substrate to the interdigital region. As GaAs is not transparent the gate must be activated by illumination through the test circuit. This places a serious limitation on the utility of the bulk LT GaAs probe. Nevertheless the probe has been used to both launch and detect picosecond voltage transients.

4.1. Time and voltage resolution of bulk probes

To test the high-speed performance of these probes a test structure was defined on damaged SOS as shown in Fig. 7. The device under test consisted of a coplanar transmission line with $20\ \mu\text{m}$ electrode width separated by a $20\ \mu\text{m}$ gap. A test signal was generated by PC switching between the electrodes on the semitransparent SOS sample [18].

The experiment was aligned by viewing the probe through the SOS sample. This allowed the probe and sample substrates to be brought into close parallelism by observing fringes caused by partial reflections from these surfaces. A multimeter was then used to determine contact by measuring resistance through the PC switch. The signal generating beam, or pump beam, was focused onto the PC gap on the SOS-based circuit, while the probe-gating beam, or probe beam, was focused through the SOS sample onto the back side of the probe's PC switch. The average gate resistance with the probe beam on was typically between 0.1 and $10\ \text{M}\Omega$ and several hundred megohms without. The delay of the probe beam was adjusted by means of a computer-controlled optical delay stage to scan through the waveform in time. Charge was collected by the probe during the sampling intervals and fed by coaxial cable to a lock-in amplifier. To differentiate signal from dark current and other sources of noise the pump beam was chopped at the lock-in frequency. Data were taken with the probe at a point $100\ \mu\text{m}$ away from the signal generation switch. The results, shown in Fig. 8, were a $2.3\ \text{ps}$ full-width at half-maximum (FWHM) response-time and a sensitivity of a few microvolts per square root hertz. With a repetition rate of $100\ \text{MHz}$, this sensitivity corresponds to $10\ \text{mV}$, i.e. a single shot. The laser used to make this measurement had a fixed repetition rate of $100\ \text{MHz}$ and delivered $>100\ \text{pJ}$ per pulse in each beam.

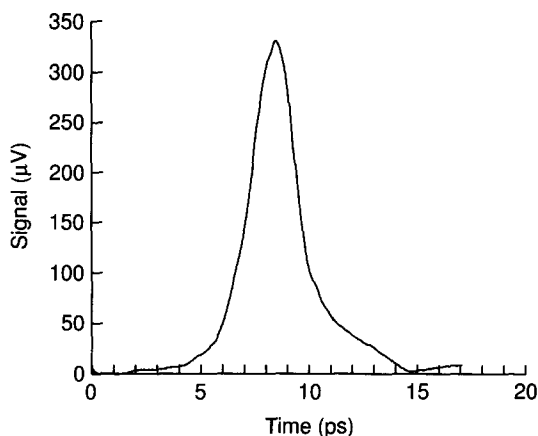


Figure 8 Impulse response of the rigid LT GaAs probe. The test signal is generated by a 100 fs optical pulse via the photovoltaic effect in SOS.

4.2. Mechanical properties of the bulk probes

At the time of these experiments attempts were made to determine the repeatability of the contact made by the probes with $3\ \mu\text{m}$ -base sharp tips. These attempts were unsuccessful because the stability of control, combined with the lack of good adhesion between Ti and Au, caused the tips to break away from the surface. Larger contact pads typically maintained good adhesion. When the pads broke free they were generally found adhering to the device under test. One damaged probe showed a crater where Ti had been in contact with LT GaAs. One could not judge from the scanning electron micrographs of this area whether the damage was caused by direct force or by ohmic heating. Nevertheless the strong adhesion of Ti to LT GaAs was noted and subsequent work was generally 100% Ti in composition. Further work with all Ti metallizations in flexible probes has yielded no loss of tips due to adhesion problems, so it may be concluded that the scanning force probes do not allow sufficient force to break the metal from the LT GaAs surface. More recent measurements by Pfeifer [21] show the utility of probes formed with silver epoxy tips on SOS.

4.3. Contact measurements with bulk probes

Contact repeatability in the measurements made with large tip areas ($8\text{--}20\ \mu\text{m}$) was determined by taking repeated traces in the same location, lifting the probe and replacing it between measurements. This type of measurement indicated that repeatability on the order of 10% was rather difficult. This difficulty rests primarily in the ability to maintain identical illumination conditions as the experiment proceeds. Direct measurements of contact resistance must be made through a $10^9\ \Omega$ switch resistance, making accurate determination of the resistance of the tip sample junction impossible.

While the sensitivity of the first probe and its speed were very good, the inability of the probe to measure anything but a transparent device was a serious problem. To remedy this difficulty SOS was used to make probes following the same guidelines used in making the LT GaAs probe. The new, more versatile probe, exhibited a 2.1 ps response and a similar minimum detectable voltage.

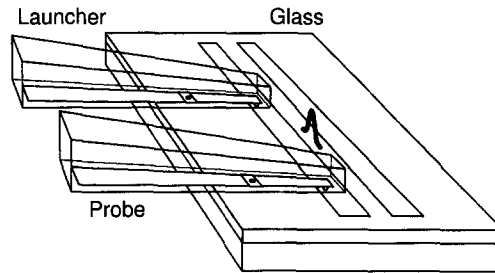


Figure 9 Configuration of two probes to launch and detect a signal on an arbitrary substrate.

4.4. Launching and detecting signals with bulk PC probes

With both the LT GaAs and the SOS probes experiments have been done to show the utility of the probes in high-speed measurement of analogue and digital devices [18–22]. To test the probes' ability to launch and detect signals, two probes are fashioned with tips at left and right corners, respectively. This allows measurement of the generated signal to be made by the sampling probe with minimal propagation distance. This system is connected as follows: the launching probe is biased to 1 V direct current (d.c.); a transmission line formed on a glass substrate is shorted at the end and grounded; and the output of the sampling probe is connected to a lock-in amplifier. The pump beam is directed at the launching probe's gate through the glass sample and chopped at the lock-in frequency. The probe beam is focused onto the switch of the sampling probe through the device under test.

Figure 9 shows the two probes placed near each other with their pads in contact with the coplanar strip transmission line on glass. Waveforms are acquired from both the signal line and the ground line with the launching probe both crossing the ground line and not crossing. The data taken on either line displayed a surprising long-duration shoulder (tens of picoseconds), but the onset of the signals was different from the signal line to the ground. Taking the difference of these signals produced a trace with a few picoseconds resolution. Consistent measurements are obtained by careful alignment of the switching beams on the probe switches. The waveform shown in Fig. 10 was found by normalizing and subtracting the signals measured on the ground and signal conductors at a distance of $400\ \mu\text{m}$ from the signal generation point. The normalizing factor varied between one and two and was chosen to produce a difference of zero signal in the range of 20–30 ps from the onset of the pulse. Experimentally this is a time-frame where no reflections are expected to occur. The source of the long-duration shoulder is still unclear. When the experiment was repeated with micrometre-thick, flexible probes these shoulders did not appear.

4.5. Measurements of microwave circuits using bulk PC probes

Engineers in the area of high-frequency microwave and millimetre wave electronics currently use network analysers to perform measurements of *S*-parameters up to 110 GHz. High-speed responses may also be measured by sampling oscilloscopes with temporal resolution down to about 20 ps. External PC sampling can be applied to overcome some of the major limitations of these instruments. The first advantage of using the external probe is its speed. Its 1 ps temporal resolution makes it faster than its electronic counterpart. Second, the PC probe has high impedance, allowing measurements to be made on devices which cannot be terminated

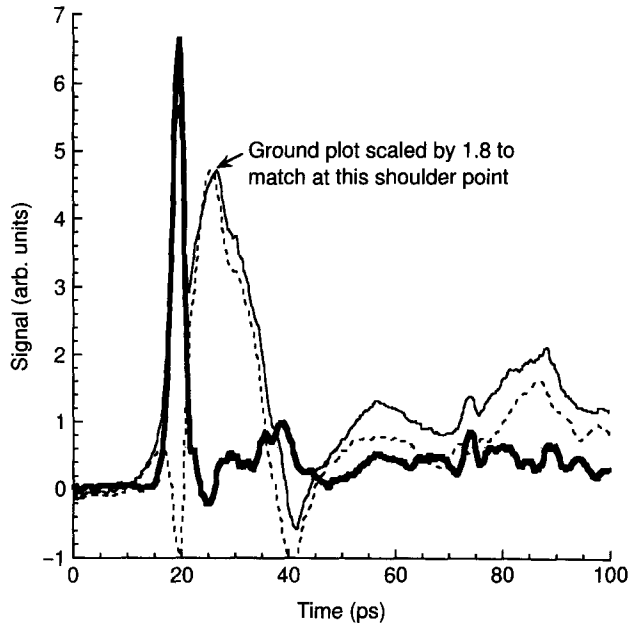


Figure 10 Signal launched and detected by probes contacting a circuit on a glass substrate. The signal shown is the difference (—) between waveforms measured on (—) signal and (---) ground conductors of a coplanar strip transmission line. A scaling factor was applied to one measurement to eliminate d.c. offset.

into the conventional $50\ \Omega$ oscilloscope port. The flexibility of the PC probe allows it to be moved around to different parts of an operating circuit. Finally, testing the internal operation of a circuit is not possible with conventional sampling oscilloscopes or network analysers.

To test the use of the PC probe in millimetre-wave electronics [18, 22] a test-bed fabricated on an LT GaAs substrate was used. This circuit consisted of a microstripline designed for 90–180 GHz operation in a frequency doubler. A $70\ \mu\text{m}$ wide microstripline and band block filter were fabricated on an LT GaAs sample with $100\ \mu\text{m}$ thickness. In addition to the millimetre-wave circuit a PC gate was formed on the transmission line to allow the formation of picosecond pulses using 120 fs pulses from a Ti:sapphire laser. The PC probe was formed from an SOS sample with a contacting pad of several micrometres diameter.

This experiment is aligned and contact resistance is monitored to determine contact with the device under test. The signal generating beam is focused onto the PC gap on the LT GaAs-based circuit, while the probe beam is focused through the sapphire onto the back side of the probe's PC switch. Charge collected by the probe during the sampling intervals is conducted by coaxial cable to a lock-in amplifier. The pump beam is chopped at the lock-in frequency to differentiate signal from dark current and other sources of noise. Waveforms taken with the probe at the input to the band-block filter and at the output, as indicated in Fig. 11, are recorded. Fourier transforms of these waveforms are taken, and their ratio corresponds to the S_{21} spectrum shown in Fig. 12. The unique ability of the probe to measure internal points on a device is shown in that it can be used to measure the resonance on the radiating section of a band-blocking filter. In Fig. 13 the 90 GHz resonance of the filter can be seen.

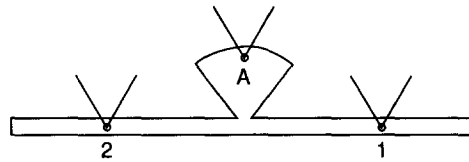


Figure 11 Diagram of a millimetre wave band-blocking filter, showing locations of test points (1 and 2) for S_{21} measurement and point (A) for measurement of the radiating signal on the pie-section.

This demonstrates the basic concept of s -parameter characterization using external PC probes. Further work on stabilization of optical alignment and electrical contact is necessary to make a functional tester with this technology. With current developments in compact diode-pumped lasers there is a much greater opportunity to develop commercial instrumentation of this type.

4.6. Testing high-speed logic with a PC probe

In a similar experiment [22] a 30 ps switching time is measured for an enhancement–depletion-mode (E–D-mode) InAlAs–InGaAs heterostructure insulated gate field effect transistor inverter using an LT GaAs probe. A large contact point is again used to avoid tip breakage from the forces applied by the bulk support. In this experiment an SOS test fixture is used because of its transparency. Unlike the s -parameter measurement, however, the device for this test is bonded into place onto its test fixture. This fixture was a modified coplanar stripline section on an SOS substrate. The modifications made to these transmission lines were the addition of pulse generation sites and the placement of d.c. bias pads. The E–D HIGFET inverter test signal was measured on the transmission lines near the input bond and the output bond to determine the gate delay. The measured signal shows a 40 ps delay. Accounting for delays in the wire bonds, the response of the logic device is found to be less than 30 ps.

By measuring the ultimate speed of the bulk external PC probe and by using it for testing various structures and devices one is assured that this probing technology has capabilities similar to those found in electrooptic sampling. One also finds a significant advantage in sensitivity with the bulk probe. In an effort to overcome the difficulties in alignment of the

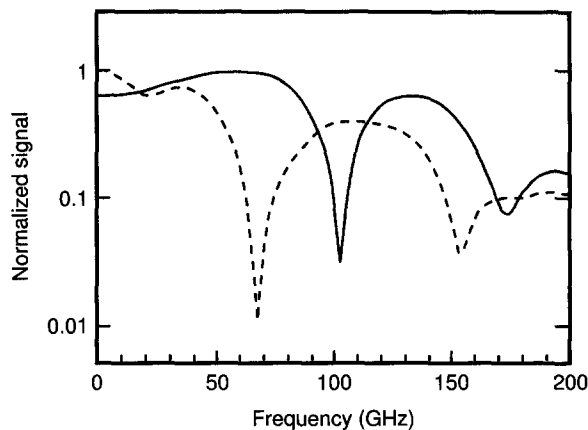


Figure 12 S_{21} as measured on an 80 and 100 GHz band-blocking filter. Dips in S_{21} indicate actual operation at 70 and 100 GHz.

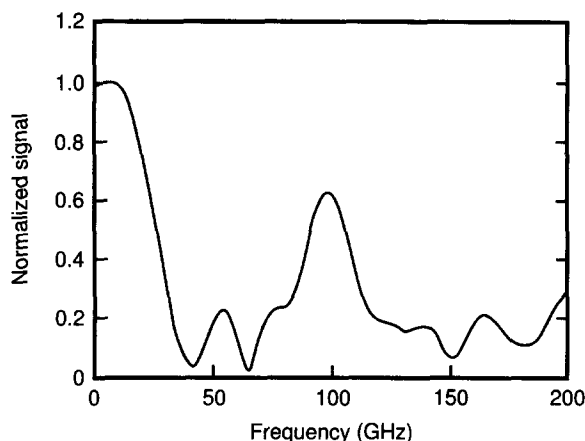


Figure 13 Fourier transform of the signal measure at point A on 90 GHz filter in Fig. 11.

optical beam and the consequent uncertainty in measurements the authors have begun using cemented optical fibres to eliminate drift in signal calibration.

4.7. Comparison of noise figures for LT GaAs probes and SOS probes

Measurements made on transparent substrates with LT GaAs probes yield noise on the order of $4 \mu\text{V Hz}^{-1/2}$. In comparison, SOS probes used to test arbitrary circuits display a comparable noise figure. As mentioned in [20] these figures are dominated by laser noise. Advances in these numbers may be expected with the elimination of photovoltaic signals from the gate and with the use of diode-pumped lasers. In the first case the coupling between the noise source and the measurement system is reduced. In the second case noise is addressed at the source; the ultrafast laser pump.

5. Fabrication and mounting procedure for LT GaAs cantilever probes

The basic elements of the PC SFM probe are three: contacting tip, PC switch and flexible cantilever. It is also necessary to support these elements in such a way as not to interfere with the sensor which detects flexure of the cantilever. The first two of these elements, the tip and the switch, can be made so small that they would be invisible to the eye. To make this portion of the system would involve defining a $5 \mu\text{m}$ diameter mesa on an LT GaAs–AlGaAs–GaAs substrate isolating the LT GaAs layer. A self-terminated tip would be formed on the mesa with a metal (other than Ti) not etched by buffered HF (BHF). The tip and LT GaAs would then be freed by dissolving the AlGaAs in BHF.

The next most favourable approach has been to copy the basic design geometry of the commercial probes, using LT GaAs as the cantilever material [23]. This method has been used successfully in two basic ways. In one case the cantilever is supported by its own GaAs substrate. In the other case the cantilever epilayer is mounted on an independent substrate.

The fabrication procedure is identical for the two approaches, to the point where the cantilever is freed from its host substrate. The common processing steps are as follows:

- (a) The LT GaAs and AlGaAs are etched to define the perimeter of the probe.
- (b) A metal layer is defined by photolithography, which includes the PC switch and leads in one direction to the tip and in the other to the external electronics.

- (c) The tip is formed by self-terminating lift-off.
- (d) The GaAs wafer is thinned to $100\ \mu\text{m}$ by lapping.
- (e) The front side is protected by black wax.
- (f) The back side is etched down to the AlGaAs.

In making cantilevers supported by GaAs, Au is patterned on the back side to protect the bulk portion of the probe from the etchment used to free the cantilever portion. The $100\ \mu\text{m}$ thick sample is covered on the front by black wax to protect exposed LT GaAs and GaAs from the $\text{NH}_4\text{OH}:\text{H}_2\text{O}$ etchant. This etch is the most critical of the processes in the probe fabrication. If the black wax does not seal the thin linear path along the AlGaAs at the probe perimeter the back-side etch will begin to dissolve the support for the tip on the front side. Figure 14 illustrates the probe embedded in protective black wax, while the native wafer is removed by etch. This problem can be avoided by leaving $100\text{--}200\ \text{nm}$ of AlGaAs in the bottom of the front-side etch-trough. This layer acts to stop the $\text{NH}_4\text{OH}:\text{H}_2\text{O}$ etch and does not provide enough mechanical strength to prevent the probes from separating. After the etch removes the exposed GaAs and the black wax is dissolved in trichloroethylene (TCE), the LT GaAs extends from the GaAs base as a cantilever. The resulting probe is shown in Fig. 15.

Once the fabrication process is completed the probes are mounted in the same way as a conventional probe, but a thin wire is also connected to the output of the probe with silver epoxy. The mechanical properties of this probe will be discussed in the next section.

As mentioned, the authors have also made probes which are supported by foreign substrates. This process eliminates the thinning and the back-side patterning of the previous method. When the front side is protected by black wax and $\text{NH}_4\text{OH}:\text{H}_2\text{O}$ is used to dissolve the substrate, epitaxial layers of LT GaAs–AlGaAs remain. When the black wax is removed in TCE $1.5\ \mu\text{m}$ thick LT GaAs/AlGaAs sheets $1 \times 5\ \text{mm}$ are left in solution. Contaminated solvent is decanted repeatedly and finally replaced with ethanol (ETOH) for storage. Epitaxial crystals which have been separated from their host substrate are stored in ETOH, as they will bond strongly to smooth surfaces if allowed to dry.

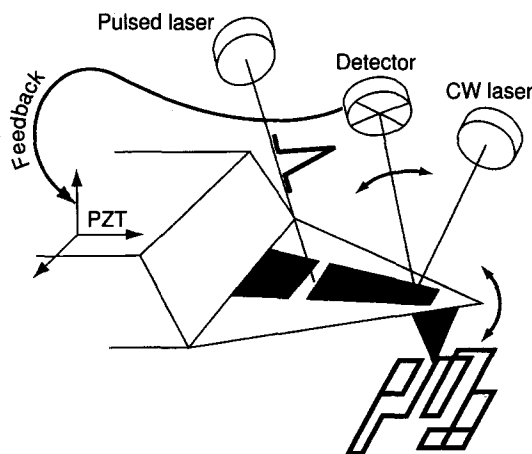


Figure 14 Configuration of PC SFM probe. The CW laser and position-sensitive detector provide feedback for imaging, while the pulsed laser induces the PC gate to sample a point on the unknown waveform. (PZT: piezoelectric transistor.).

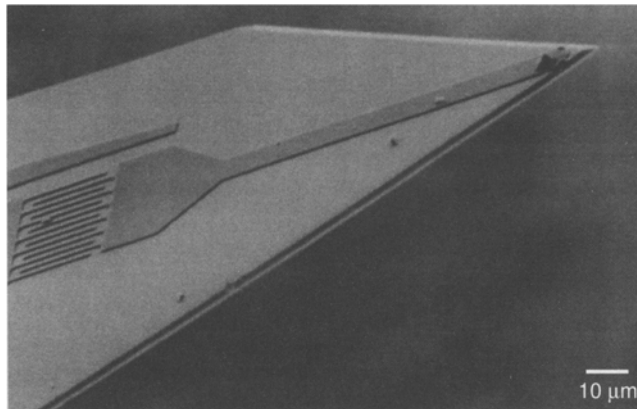


Figure 15 Scanning electron micrograph of the PC SFM probe. The thickness of the cantilever is $1.5\ \mu\text{m}$ and the tip-gate distance is about $100\ \mu\text{m}$. The flexibility of this probe prevents the tip from breaking away from the probe.

Probes are assembled in the following way. Each sheet is removed from the ETOH bath by dropper and placed on a sheet of card paper to dry. Once dry the epifilm is released from the surface tension of the ETOH and is free to be turned over with a fine needle. The LT GaAs–AlGaAs crystal is placed probe-tip-down on the card. A stripe $\sim 0.1\ \text{mm}$ wide of low viscosity UV-curing cement is painted length-wise onto the largest face of a block of glass $0.5 \times 2 \times 3\ \text{mm}$ in size. The block is then inverted and lowered with tweezers onto the epicrystal so that the probe cantilevers extend over the ends of the block. As the block nears, the probe sheet clings to the surface of the glass block and surface tension causes the stripe of cement to migrate over the entire contact area of the block-probe overlap. The UV-cement need not be cured as the surface tension is strong enough to prevent the probe from being moved after the wetting process occurs.

In order to allow fibre coupling to the probe glass blocks have been prepared with a groove in the face opposite the probe as shown in Fig. 16. A fibre is then prepared with a 45° facet on the end causing total internal reflection to direct light perpendicular to the fibre axis with a spread angle $< 10^\circ$. The fibre is laid on the ferromagnetic base used to mount the commercial probes. Using a microscope the probe block is placed groove down on the fibre and cemented in place with a very small amount of ‘super glue’ which is applied to tack the chip in place. This allows the fibre the freedom to slide and rotate. Using such adjustment, light coupled through the fibre is directed to the probe’s switch and the fibre is cemented in place. Silver epoxy is then used to attach a wire to the output end of the probe.

5.1. Mechanical properties of the SFM probes

The mechanical properties of the LT GaAs probes are derived from the nature of the LT GaAs crystal and the metals evaporated on its surface. There are a few surprising properties of the epicrystals which stem from the fact that they have a very high length-to-thickness ratio and very low weight. In the process described above, the $1.5\ \mu\text{m} \times 1 \times 4.5\ \text{mm}$ crystal is 3000 times longer than it is thick. While ratios of this kind are usually found in plastics and metals it is rare to think of crystals with such dimensions. This aspect ratio is what gives rise to the flexibility of the probe. While it is made of a ‘brittle’ material the $200\ \mu\text{m}$ long cantilever is capable of bending 90° up or down without breaking. This flexibility is an advantage in the

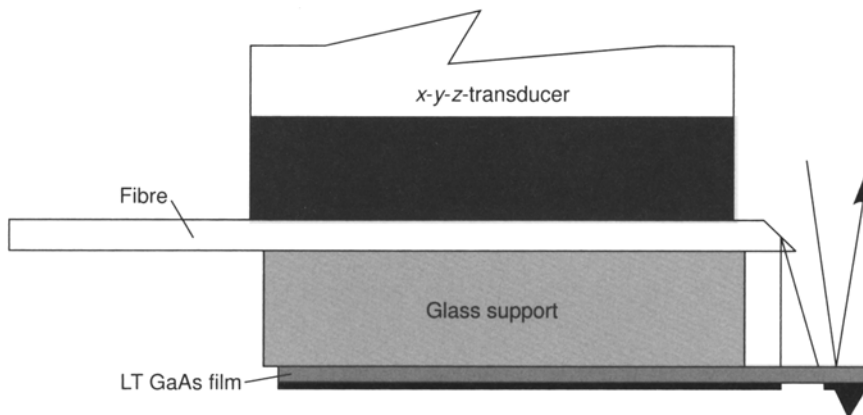


Figure 16 Schematic of the PC SFM probe mounted with fibre-optic gate-beam delivery to allow scanning of the probe without misalignment.

survivability of the probe. The authors have not been able to remove tips from these cantilevers because it was not possible to apply enough force to the material to do so. The force constant for the $200\ \mu\text{m}$ triangular cantilever with $400\ \mu\text{m}$ base is within a factor of two of the force constant of the more flexible of the commercial probes. This is measured by pressing an LT GaAs probe against a commercial probe with known force constant and gauging the relative deflection of the two cantilevers. This places the spring constant of the LT GaAs probe at about $1\ \text{nN nm}^{-1}$.

5.2. Performance of two scanning force PC probes

Probes of both the types mentioned above have been used to measure signals on high-speed structures. The GaAs-based probe is used in measuring the temporal response of the probe in a manually controlled positioning fixture, while the glass-based probe is used to make fibre-coupled measurements under the control of a commercial scanner.

5.2.1. Temporal resolution

In measurements of temporal resolution the LT GaAs probe is lowered into contact with one electrode of a coplanar strip transmission line on LT GaAs (see Fig. 17). A 100 fs pulse laser beam is used to excite a subpicosecond electrical pulse on the transmission line, while another beam is delayed and focused onto the probe's switch to sample the impulse. The delay is controlled and the waveform recorded by computer. The resulting waveform, Fig. 18, demonstrates a minimum detectable voltage of $10\ \mu\text{V Hz}^{-1/2}$ and a risetime of 2.5 ps. Due to the difficulty in reflecting beams to the gate inside the commercial scanning microscope the ultimate resolution of the probe is not operated in the scanning fixture. To determine the effect of electrical measurements on the probe's ability to acquire an image the probe was removed from the time-resolved measurement apparatus and placed in the commercial scanner. The image resulting from a scan of a test pattern indicates that submicrometre imaging capability is retained.

5.2.2. Integrated scanning force microscope and PC sampling probe

The measurement of waveforms in conjunction with imaging is achieved by placing the fibre-coupled probe in the commercial scanning system and imaging a coplanar transmission line on

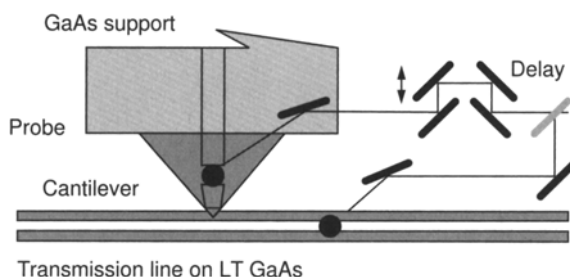


Figure 17 Schematic of the PC SFM probe impulse response measurement.

LT GaAs. A 30 cm optical fibre is used to deliver pulsed light to a PC gap in the line, creating a test signal. When imaging is completed the probe is placed in the desired location on the transmission line and the transient waveform is measured. Though the measurement is currently limited to 5 ps by the dispersion of the 100 fs laser pulse in 30 cm of single mode fibre, the noise characteristics are similar to those obtained with 100 fs gate pulses.

5.2.3. Imaging capabilities

The spatial resolution of the PC SPM may be stated in terms of the probe's ability to measure surface roughness and in terms of its ability to measure edge features. In regard to the finest dimensions a scanning electron micrograph (SEM) shows the point of the tip to have a radius of curvature of less than $0.1 \mu\text{m}$. In agreement, images scanned by the probe display surface roughness at the order of 25–50 nm. SFM images indicate an angle included by the probe tip of about 60° . This allows the probe to make measurements on slopes of less than 60° inclination. A topographic scan of an Au grid with $2 \mu\text{m}$ squares and $1 \mu\text{m}$ troughs is shown in Fig. 19.

5.2.4. Contacts and contamination

Following high-speed measurements to test the feasibility of ultrafast PC SFM a study was done to measure the effectiveness of the probe in making d.c. contact with devices. The surprising result was that, while picosecond transients were readily measured, there was a

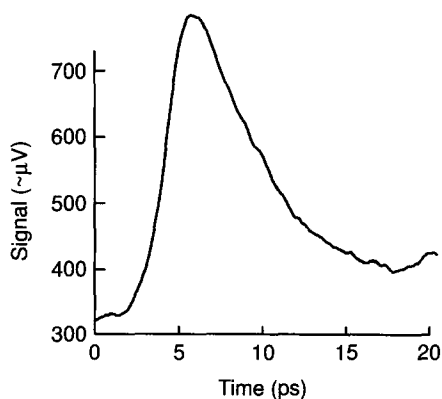


Figure 18 Impulse response of the PC SFM probe. This measurement indicates microvolt resolution, but contains an unexplained d.c. offset.

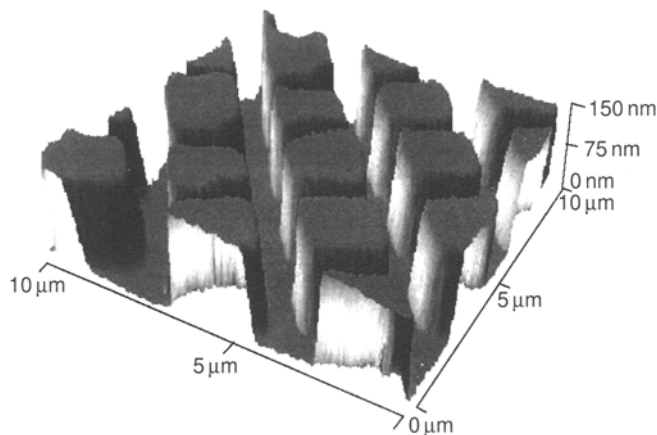


Figure 19 Image scanned by the PC SFM probe after measurement of impulse response. The test structure has $1\ \mu\text{m}$ troughs with $2\ \mu\text{m}$ squares, nominally $130\ \text{nm}$ high.

great deal of variability in the probe's d.c. contact to the test circuit. The test involved illuminating the PC SFM probe with CW light to increase its conductivity, and scanning the probe across the surface of Au and Al structures to observe areas of contact. In this experiment portions of the test circuit are biased with a sinusoidal voltage at $1\ \text{kHz}$ and the probe is connected to a lock-in amplifier to measure current at that frequency. The image representing contact is compared to the topographic image which is acquired simultaneously. Ideally the d.c.-conductivity image would indicate a particular current for all points over the 'live' metal areas and no significant signal elsewhere. The results reveal that much of the sample does not allow d.c. contact under the conditions of force and voltage used in the experiment and that some areas allow contact on the forward pass and not on the reverse pass. The results further indicate a higher probability of contact at points on the perimeter of a metallization than at points on the surface. These results are similar for Au and Al samples. The range of possible explanations includes sample contamination, tip contamination and oxidation of the tip. Oxidation of the sample is ruled out by the use of an Au sample. Presently, contamination appears to be the most likely candidate due to the non-uniformity of the result. Although picosecond measurement does not appear to have the level of variation in contact observed in these d.c. measurements, a complete scan acquiring waveforms at each point has not yet been done to test more thoroughly.

5.3. Voltage measurement using a semiconductor laser

While the last few years have seen great advances in short-pulse solid-state laser technologies, most of these lasers cannot be locked to an arbitrary clock. In order to test circuits which have internal clocks or clock rates which vary the authors use a commercial gain-switched semiconductor laser [24]. This laser provides $30\ \text{pJ}$ pulses of $100\ \text{ps}$ duration at $800\ \text{nm}$. The drive electronics accept transistor-transistor logic (TTL) trigger signals and maintain a jitter of $50\text{--}100\ \text{ps}$. Figure 20 shows the configuration of test electronics used to acquire time-resolved signals using PC SFM sampling. The data in Fig. 21 show measurements of $4\ \text{V}$ signals on a test integrated circuit plane and on a $1.5\ \mu\text{m}$ conductor. Using this method of testing one is able to resolve signals of $2\ \text{V}$ with a single laser shot. Based on the average current taken from the test circuit, $5\ \text{fC}$ of charge was removed per shot.

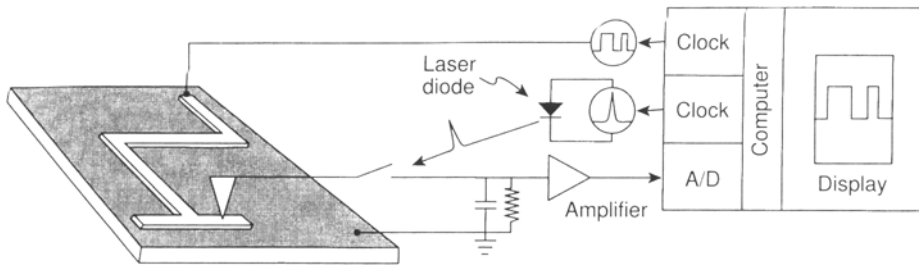


Figure 20 Schematic of the system used to test integrated circuits with arbitrary repetition rate.

5.4. Barriers to PC SFM

Much of the data taken with the variety of probes covered in this paper suggest that the PC probe technology is a good choice for interrogating the internal working of circuits. A better knowledge of the effects of surface contamination and of what constitutes sufficient force to make contact is a clear path for investigation in the reliability of this technology. Likewise, an understanding of the difference between the sampling measurements made by bulk probes and by micrometre-thick probes could help to explain the origin of the offset in the voltage waveforms acquired with the cantilever probes.

6. Conclusions

The authors have fabricated SFM probes from LT GaAs using common tools of microfabrication, and have demonstrated 100 nm spatial resolution, 2.5 ps temporal resolution, or better, and few microvolts per square root hertz. In the investigation of the PC effect one found the LT GaAs material system to be a highly effective gate material for application to integrated circuit testing. In circumstances where a rigid probe is desired and a transparent substrate is necessary, damaged SOS is a suitable replacement. Both materials produce slightly greater than 2 ps temporal resolution and sensitivity in the first decade of the microvolt per square root hertz range.

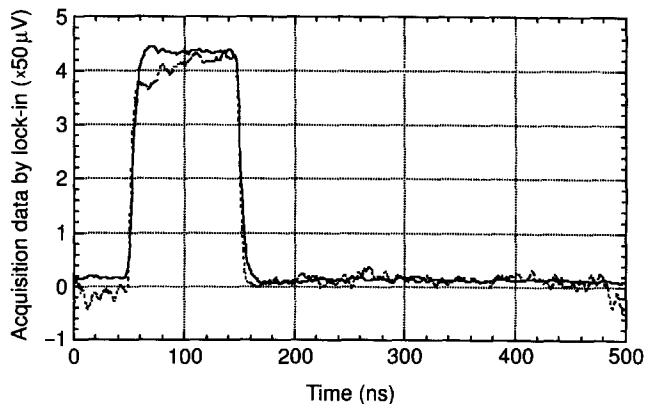


Figure 21 Waveforms sampled by laser diode-based PC SFM. The measured signal is 100 ns in duration and 4V in amplitude: (—) on the plane, (----) on the finger (1.5 μm).

The authors anticipate expanding interest in the use of photoconductivity as a mechanism for gated sampling measurements in the picosecond regime, with applications in circuit testing and in the study of mesoscopic structures and devices.

Acknowledgements

This work is the product of many researchers at the University of Michigan and at Fujitsu Laboratories. Steven Williamson, now President of Picometrix Inc., pioneered the LT GaAs MSM work with the help of Yi Chen, who is now at AT&T. Joungho Kim, who is now at Samsung, fabricated and tested bulk LT GaAs and SOS probes on analogue and digital systems. Many important contributions to the understanding of the LT GaAs material system were made by Frank Smith, John Whitaker, Heng-Ju Cheng (Picometrix), Hsi-Huai Wang and Jiunn-Ren Hwang.

Support for the development of VLSI testing was received under contract with FUJITSU Laboratories Ltd. This work was also supported by a grant from the National Science Foundation through the Center for Ultrafast Optical Science under STC PHY 8 920 108. Additional support was granted by the SDI programme through the Army Research Office under DAAL-0392G-0294.

References

1. S. CONCIONA and N. RICHARDSON, in *Proceedings of the International Test Conference* (IEEE Computer Society Press, Silver Springs, MD, 1987) p. 554.
2. S. GORLICH, H. HARBECK, P. KESZLER, E. WOLFGANG and K. ZIBERT, in *Proceedings of the International Test Conference* (1987) p. 566.
3. J. A. VALDMANIS, in *Measurement of High-Speed Signals in Solid State Devices*, edited by R. B. Marcus (Academic Press, San Diego, 1990) p. 135.
4. J. A. VALDMANIS and G. A. MOUROU, *IEEE J. Quantum Electron.* **QE-22** (1986) 69.
5. U. D. KEIL and D. R. DYKAAR, *OSA Proceedings on Ultrafast Electronics and Optoelectronics*, Vol. 14, edited by J. Shaw and U. Mishra (Optical Society of America, Washington DC, 1993) p. 189.
6. K. DeKORT and J. VREHEN, *Microelectron. Eng.* **16** (1992) 341.
7. A. HOU, B. NECHAY, F. HO and D. BLOOM, *Opt. Quantum Electron.* **28** (1966) 819.
8. D. H. AUSTON, in *Picosecond Optoelectronic Devices*, edited by C. H. Lee (Academic Press, London, 1984).
9. D. R. GRISCHKOWSKY, M. B. KETCHEN, C.-C. CHI, I. N. DULLING III, N. J. HALAS and J. M. HALBOUT, *IEEE J. Quantum Electron.* **24** (1988) 221.
10. F. W. SMITH, H. Q. LE, V. DIADIUK, M. A. HOLLIS, J. M. CHWALEK, S. GUPTA, M. Y. FRANKEL, D. R. DYKAAR, G. A. MOUROU and T. Y. HSIANG, *Appl. Phys. Lett.* **54** (1989) 890.
11. S. GUPTA, S. L. WILLIAMSON, Y. CHEN, J. F. WHITAKER and F. W. SMITH, *Laser Focus World*, June (1992).
12. J. KIM, S. WILLIAMSON, J. NEES, S. WAKANA and J. WHITAKER, *Appl. Phys. Lett.* **62** (1993) 2268.
13. Y. CHEN, S. L. WILLIAMSON, T. BROCK, F. W. SMITH and A. R. CALAWA, *Appl. Phys. Lett.* **59** (1991) 14.
14. J.-R. HWANG, H.-J. CHENG, J. F. WHITAKER and J. V. RUDD, *Opt. Quantum Electron.* **28** (1996) 963.
15. J.-R. HWANG and J. F. WHITAKER, in *Proceedings of the Annual Meeting of the Lasers and Electro-optics Society* (IEEE, Piscataway, NJ, 1995) paper UOE1.3, p. 331.
16. J. B. D. SOOLE and H. SCHUMACHER, *IEEE Trans. on Electron Devices* **37** (1990) 2285.
17. C. A. SPINDT, I. BRODIE, L. HUMPHREY and E. R. WESTERBERG, *J. Appl. Phys.* **47** (1976) 5248.
18. J. KIM, J. SON, S. WAKANA, J. NEES, S. WILLIAMSON, J. WHITAKER and G. A. MOUROU, *OSA Proceedings on Ultrafast Electronics and Optoelectronics* Vol. 14, edited by J. Shaw and U. Mishra (Optical Society of America, Washington DC, 1993) p. 224.
19. D. DYKAAR and S. B. DARACK, *Appl. Phys. Lett.* **65** (1994) 2525.
20. T. PFEIFER, H.-M. HEILIGER, E. S. KAMIENSKI, H. ROSKOS and H. KURTZ, *J. Opt. Soc. Am. B* **11** (1994) 2547.
21. T. PFEIFER, H.-M. HEILIGER, H. ROSKOS and H. KURTZ, *IEEE Trans. Microwave Theory Tech.* **43** (1995) 2856.

22. J. KIM, Y.-J. CHAN, S. WILLIAMSON, J. NEES, S. WAKANA, J. WHITAKER and D. PAVLIDIS, in *IEEE GaAs IC Symposium* (IEEE, Piscataway, NJ, 1992).
23. J. NEES, S. WAKANA and C.-Y. CHEN, *Ultrafast Phenomena IX*, edited by P. F. Barbara, W. H. Knox, G. A. Mourou and A. H. Zewail (Springer-Verlag, Berlin, 1994) p. 139.
24. J. NEES, S. WAKANA and S. HAMA, *Ultrafast Electronics and Optoelectronics*, Vol. 13, *OSA Technical Digest Series* (Optical Society of America, Washington, DC, 1995) p. 172.